Radio Propagation Measurements and WINNER II Parameterization for a Shopping Mall at 61–65 GHz

Aki Karttunen, Jan Järveläinen, Afroza Khatun, and Katsuyuki Haneda
Aalto University School of Electrical Engineering
Espoo, Finland
e-mail: katsuyuki.haneda@aalto.fi

***Abstract*—In this paper, we derive parameters for the WINNER II channel model for a shopping mall environment at 61–65 GHz for both line-of-sight (LOS) and for obstructed-line-of-sight (OLOS) . The parameters are mostly based on channel measurement results reported in this paper. Due to the large measurement bandwidth, and the highly specular nature of the channels, discrete propagation paths can be identified from the results. The parameterization is based on the measured large scale parameters and representation of each propagation path by a single cluster.**

Keywords—channel measurement, channel model, 60 GHz, WINNER

I. Introduction

Due to large available bandwidths, e.g., at the 60-GHz range, millimeter wave bands are predicted to play an important role in providing higher data rates in future fifth generation (5G) systems. In this paper, we present parameterization for the popular WINNER II channel model [1] for the 60-GHz range based on channel measurements in a shopping mall.

WINNER II is a geometry-based stochastic channel model (GSCM) that is parameterized for many scenarios at the microwave frequencies [1]. It aims to reproduce the physical parameters of plane waves by creating imaginary scatterer distribution from statistical distributions of the channel parameters. The scatterer distribution is created with angles of departure and arrival and delay of each scatterer seen from the transmitter (Tx) and receiver (Rx) antennas. The WINNER II channel model is popular in modeling the channels at microwave frequencies due to a reasonable compromise between accuracy and complexity.

To the best of authors' knowledge, this is the first time WINNER II has been parameterized for 60 GHz. A wide range of channel measurements and modeling work for 60 GHz and other frequencies in the millimeter wave range are reported in the literature, e.g., [2]-[7]. The narrowband microwave frequency WINNER II model may not be applicable for wideband millimeter wave modeling, which may be the main reason why WINNER II has not been parameterized for 60 GHz before.

In this paper, WINNER clusters are used to represent individual identifiable multipaths. The structure of the channel model is not changed. The channel sounder and the propagation channel measurements in a shopping mall are presented in Section II. In Section III the propagation paths are detected from the measured channels and the WINNER II channel parameters are derived and presented in Section IV.

II. Radio Propagation Measurements

A. Channel Sounder

The RF part of the ~~used~~ measurement system is illustrated in Fig. 1. The system is based on a vector network analyzer (VNA) with an intermediate frequency (IF) of 5–9 GHz. The RF frequencies 61–65 GHz are generated with up and down converters and a local oscillator (LO) operating at 14 GHz. Both Tx and Rx sides are connected by cables to the VNA.

The up converter and the Tx antenna are on a rotator. A 20 dBi standard gain horn is used as the Tx antenna. An omnidirectional biconical horn antenna is used as the Rx antenna. The Tx antenna is rotated in the azimuth direction from 0° to 360° with 3° steps. Three samples of the amplitude and phase are measured at each direction with 2001 frequency points. The 4 GHz IF bandwidth leads to a 0.25 ns delay resolution. A direct connection back-to-back calibration is used to compensate for the transfer function of the measurement system. Both Tx and Rx antennas have relatively narrow elevation plane radiation patterns which limits the measurements to the azimuth plane. Both antennas are vertically polarized and only the co-polarization measurements are performed.

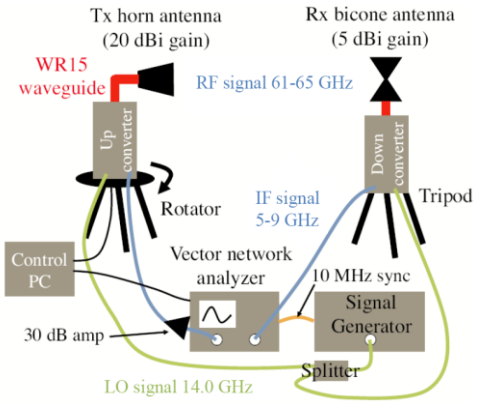

Fig. 1. Channel sounder setup for measurements at 61–65 GHz.

B. *Measurements in a Shopping Mall*

These measurements are conducted in an indoor shopping mall Sello (Leppävaarankatu 3-9, Espoo, Finland). The measurements are done on the first and on the third floors. The floor maps with the Tx and Rx locations are presented in Fig. 2 and photographs of the measurement locations are in Fig. 3. In total 54 measurements are done, 40 of them are line-of-sight (LOS) and 14 obstructed-line-of-sight (OLOS) measurements. In the OLOS measurements the Rx antenna is located behind a wide pillar which blocks the LOS component completely (see Figure 2). The Tx-to-Rx distances are between 1.5 m and 16 m. The antenna height for both Tx and Rx is 2 m. The Rx locations are considered as the base station (BS) and the Tx locations as the mobile station (MS) locations.

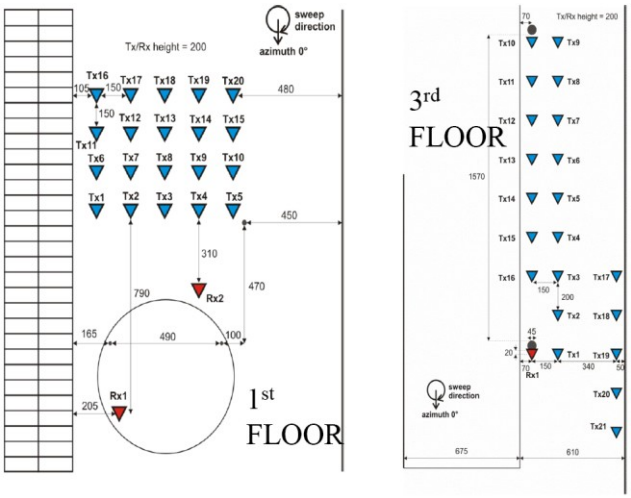

Fig. 2. Floor maps and locations of the Rx and Tx. 33 LOS measurements on the 1st floor and 7 LOS and 14 OLOS measurements on the 3rd floor.

Fig. 3. Photographs of the measurement sites at the 1st and 3rd floors of the Sello shopping mall.

III. Measurement Result Analysis

A. *PADP and PDP*

The first step of the measurements result analysis is to derive the power angular delay profile (PADP) and the power delay profile (PDP). A matrix of the channel transfer function is recorded as a function of the Tx rotation angle and as a function of the frequency. Then the PADP is obtained via Fourier transform from the channel transfer matrix. The Hamming window function is used over the frequency to reduce the time-domain sidelobe-level. The PDP is derived by the marginal integral of the PADP over the Tx rotation angles. An example of a measured PDP is presented in Fig. 4.

B. *Propagation Path Detection*

Propagation paths are defined as individual identifiable multipaths which originate from specular propagation mechanisms. Propagation path detection is done in a similar manner in [7]. Propagation path detection is done from PDP in order to avoid two-dimensional peak-detection from the PADP. Propagation paths are the local maxima of the PDP identifiable by the following criteria:

$$PDP(\tau) > \frac{1}{\Delta}\int_{\tau-\Delta/2}^{\tau+\Delta/2} PDP(t)\,dt, \quad (1)$$

$$PDP(\tau-\Delta\tau) < PDP(\tau) < PDP(\tau+\Delta\tau), \quad (2)$$

$$PDP(\tau) > P_n + 3dB, \quad (3)$$

$$\tau \geq d/c_0, \quad (4)$$

where Δ = 2.0 ns is the length of sliding window over delays chosen to avoid detecting artifacts and noisy peaks, P_n +3 dB is the noise threshold, $\Delta\tau$ = 0.25 ns is the delay resolution, d is the distance from Tx to Rx, and c_0 is the speed of light. The length of the sliding window, compared to the delay resolution, needs to be selected carefully in order to detect all the peaks. An example of a PDP with the detected peaks is presented in Fig. 4.

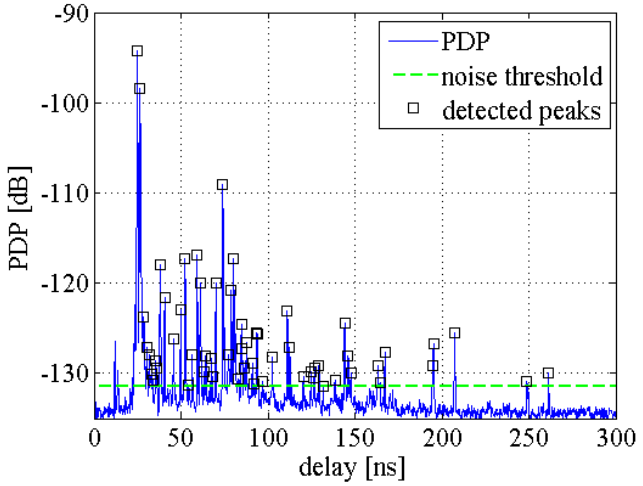

Fig. 4. Example of a PDP (solid line) and detected peaks (square markers).

After the peak detection from the PDP, angles for the detected propagation paths are found from the PADP. Finally, the path amplitudes are calculated from the path PADP amplitudes taking into account the effects of antenna gains and the windowing loss. The detected path amplitudes, delays, and angles can be illustrated in a discrete form of the PADP, as in Fig. 5.

The number of detected paths varies between 23 and 95, with an average of 65 in LOS cases. In OLOS cases, the number of detected paths varies between 11 and 31, with an average of 20. Strong paths are defined as peaks within the upper 20 dB of the PADP. The average number of strong paths is 3.6 and 9.4 in LOS and OLOS, respectively.

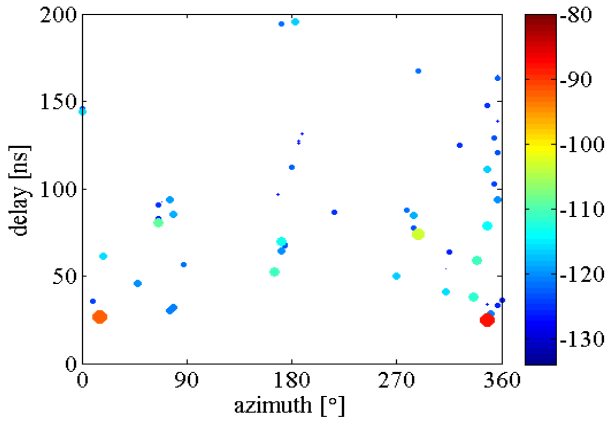

Fig. 5. Example of detected propagation paths. Both colour and marker size are used to indicate the path amplitude. Path delays are determined from PDP, angles from PADP, and amplitude from PADP taking in to account the effects of antenna gains and the windowing loss.

IV. Parameterization

The WINNER II channel model parameters are derived and collected to Tables I-V. The base station is considered to be at the Rx locations and the mobile station at the Tx locations shown in Fig. 2. Most of the parameters are derived from the measured and detected propagation paths. The 20 dB dynamic range limitation is used for the derivation of all the parameters. A brief explanation of each parameter is given in the following.

Path loss (PL) is calculated from the total sum of power in the measured paths

$$P_{tot} = \sum_{i=1}^{N} p_i, \quad (5)$$

The parameters of the distance dependent path loss model are presented in Table I. The minimum and maximum measured BS-MS distances give the applicability range of the PL model. The measured PL, PL model, and free space loss are illustrated in Fig. 6. Shadow fading is the deviation of the measured path losses from the PL model. Shadow fading standard deviations are given in Table I.

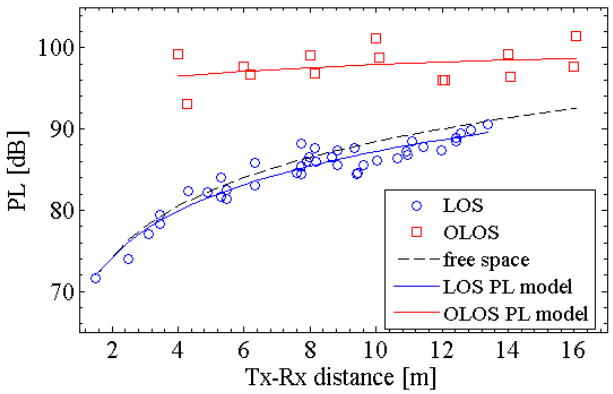

Fig. 6. Path loss.

The cross-polarization ratio (XPR) was not measured in these measurements; instead a mean XPR of 20 dB is used based on the IEEE 802.11ad channel model [2]. A standard deviation of 2 dB is used for the XPR. These are quite reasonable XPR values for millimeter wave indoor channels based on previous work by the authors [4].

The K-factor is calculated as the power ratio between the LOS component and all other detected propagation paths within the 20 dB dynamic range.

TABLE I. Parameters Derived from Path Amplitudes.

		LOS	***OLOS***
Path loss (PL) PL =A log10(d[m]) + B + C log10(fc[GHz]/5.0) + X	A	18.4	3.59
	B	68.8	94.3
	C	0	0
	X	0	0
Shadow fading (SF) [dB]	σ	1.2	2.1
BS-MS distance [m]	min	1.5	4
	max	13.4	16.1
XPR [dB]	μ	20	20
	σ	2	2
K-factor (K) [dB]	μ	7.9	N/A
	σ	5.8	N/A

Delay spread is calculated from the path amplitudes and delays as defined in [10].

In WINNER [1], the delay scaling parameter affects both maximum excess delay and the slope of the exponential delay distribution of the cluster powers. In this parameterization, the delay scaling parameter is calculated for each measurement result based on the measured maximum excess delay by approximation

$$r_\tau = t_{max}/\sigma_\tau, \quad (6)$$

where t_{max} is the maximum excess delay and σ_τ is the delay spread. The exponential delay distribution and per cluster shadowing standard deviation ζ are used to create cluster powers P_n: [1]

$$P_n = e^{\left(-\tau_n \frac{r_\tau - 1}{r_\tau \sigma_\tau}\right)} \cdot 10^{-\frac{Z_n}{10}}, \quad (7)$$

where τ_n is the normalized delay (i.e. delays after subtracting the minimum delay, see Eq. (4.2) in [1]), and Z_n = N(0,ζ) is the per cluster shadowing term in [dB]. In LOS-cases, the cluster delays τ_n in (3) need to be replaced by $\tau_n^{LOS} \cdot D$, where τ_n^{LOS} are the measured normalized path delays and D is a scaling factor that depends on the K-factor (see Eq. (4.3) in [1]). We use this definition to calculate delay scaling parameters and per cluster shadowing from the deviation of strong paths (not including LOS, since LOS is not a cluster [1]) from the exponential delay distribution in (7). The resulting single slope exponential power delay profile is used to determine the per-cluster fading by optimizing the associated distribution with log-likelihood function as in [11]. The dynamic range limit is taken into account in a similar manner as the noise level with measurement results in [11]. The average values of the delay scaling parameter and the per cluster shadowing for LOS and OLOS are reported in Table II.

TABLE II. DELAY PARAMETERS.

		LOS	***OLOS***
Delay spread (DS) log10([s])	μ	-8.28	-7.78
	σ	0.32	0.10
Delay distribution		Exp	
Delay scaling parameter	r_τ	2.5	2.0
Per cluster shadowing std ζ [dB]		2.5	5.3

TABLE III. ANGULAR PARAMETERS.

		LOS	***OLOS***
Departure angular spread (ASD) log10([°])	μ	1.09	1.61
	σ	0.43	0.11
Arrival angular spread (ASA) log10([°])	μ	1.19	1.62
	σ	0.47	0.14
AoD and AoA distribution		Wrapped Gaussian	

The angular characteristics are measured by rotating the Tx horn antenna at the MS side. The arrival angular spread (ASA) can be calculated directly from the angels and amplitudes of the detected paths. Knowing the arrival angles, excess delays, and BS and MS locations, the scattering points can be identified in *x-y* coordinates in a similar manner as in [11]. The angles of departure for each path are then derived from the BS point of view. Naturally, the assumed single-bounce propagation path condition is not valid in case of multiple reflections. Based on the measurement results the single-bounce paths dominate and the effects of misinterpreting the angles of departure of multi-bounce scatterers are acceptable. In the first floor measurements (Fig. 2) a few of the measurements show a strong double reflection from the escalator, but the location of the scatterer location is easily corrected using the image principle. A wrapped gaussian angular distribution is assumed because it is used in the WINNER channel model [1].

Cross-correlation and correlation distances of the large scale parameters are given in Table IV. The correlation distances have to be approximated from the measurement results since the smallest distance between measurement locations was 1.5 m (Fig. 2). Correlation between all parameters both in LOS and OLOS is under the limit of 1/e (≈0.37) when the distance between the measurement locations is over 2 m, therefore the correlation distances are determined solely based on the correlations over 1.5 m. A correlation distance of 2 m is used if the correlation is over 1/e. If the correlation is between 1/2e (≈0.18) and 1/e, a correlation distance of 1 m is used, and if the correlation is under 1/2e then a correlation distance of 0.5 m is used.

TABLE IV. CORRELATION PROPERTIES.

		LOS	***OLOS***
Cross-Correlation	ASD[°] vs DS[s]	0.4	0.5
	ASA[°] vs DS[s]	0.2	0.3
	ASA[°] vs SF[dB]	0.0	0.1
	ASD[°] vs SF[dB]	0	-0.1
	DS[s] vs SF[dB]	0.2	-0.4
	ASD[°] vs ASA[°]	0.0	0.0
	ASD[°] vs K[dB]	-0.4	N/A
	ASA[°] vs K[dB]	-0.3	N/A
	DS[s] vs K[dB]	-0.2	N/A
	SF[dB] vs K[dB]	0.2	N/A
Correlation distance [m]	DS [s]	1	0.5
	ASD [°]	2	0.5
	ASA [°]	1	1
	SF [dB]	0.5	0.5
	K [dB]	1	N/A

The number of clusters is defined based on the number of resulting strong clusters from the WINNER II implementation [13]. The number of clusters is optimized such that the average number of strong clusters (20 dB dynamic range) is approximately the same as the average number of measured strong paths for LOS and OLOS, i.e., about 4 and 9, respectively. For the LOS cases the addition of the LOS component (see Eq. (4.17) in [1]) needs to be taken into account and the LOS component counts as the 5th cluster.

The number of rays per cluster in WINNER II is 20. In the measurement results the paths appear to have only a single arrival/departure angle within the limitations of the measurement resolution, and therefore it can be concluded that

intra-cluster angular spread must be small. A cluster ASD and ASA of 1.5° is used.

TABLE V. CLUSTERS AND INTRA-CLUSTER PROPERTIES.

	LOS	***OLOS***
Number of clusters	4	10
Number of rays per cluster	20	20
Cluster ASD [°]	1.5	1.5
Cluster ASA [°]	1.5	1.5

Cumulative distribution functions (CDFs) of measured and WINNER II [12] delay spreads (DS) and K-factors (K) are compared in Fig. 7. The same 20 dB dynamic range is used both with the WINNER-generated clusters as with the measured paths. The model and measurements match well.

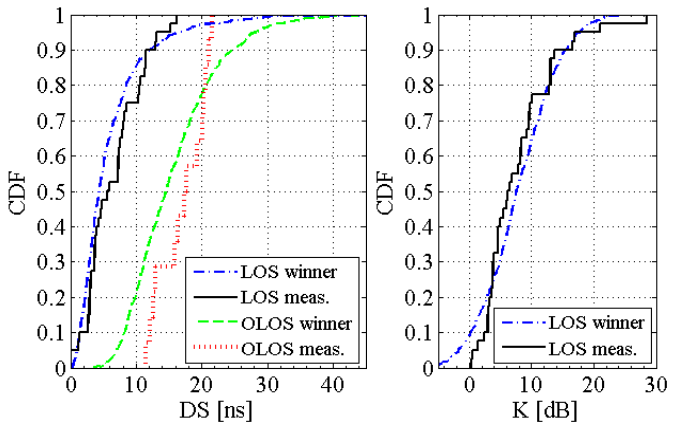

Fig. 7. Comparison of measured and WINNER II-generated LOS and OLOS DS and LOS K-factors.

V. IMPLEMENTATION ISSUES

The MATLAB implementation of the WINNER II channel model [13] defines parameters for each scenario in a file called *ScenParTables.m*. All those parameters for a shopping mall in LOS and OLOS scenarios at 60 GHz are given in Tables I-V. In addition to those parameters it is important to use '*IntraClusterDsUsed*' = 'no' and '*DelaySamplingInterval*' = 0.125 ns in a file called *wimparset.m*. Naturally, also the center frequency needs to be changed.

VI. DISCUSSION

Most of the WINNER II parameterization presented in this paper is a direct result of the measurements. The exceptions are the delay distribution, the angular distribution, and the number of rays per cluster that are considered in this work to be part of the channel model structure. The XPR mean value is based on [2], and the XPR standard deviation and the cluster ASD/ASA are educated guesses.

The validation of the derived WINNER II parameters is considered outside the scope of this paper.

VII. CONCLUSIONS

This work reported a channel measurement campaign in a shopping mall at 61–65 GHz. WINNER II parameters are presented for both LOS and OLOS.

ACKNOWLEDGMENT

Part of this work has been performed in the framework of the FP7 project ICT-317669 METIS, which is partly funded by the European Union.

REFERENCES

[1] P. Kyösti, et al., "WINNER II channel models", IST-4-027756 WINNER II Deliverable D1.1.2, V1.2.4.2, 2008, online available at [http://www.ist-winner.org/deliverables.html].

[2] A. Maltsev, V. Erceg, E. Perahia, C. Hansen, R. Maslennikov, A. Lomayev, A. Sevastyanov, and A. Khoryaev, "Channel models for 60 GHz WLAN systems," IEEE802.11-09/0334r3, July 2009.

[3] H. Yang, P. F. M. Smulders, and M. H. A. J. Herben, "Channel characteristics and transmission performance for various channel configurations at 60 GHz," *EURASIP J. Wireless Commun., Network.*, 2007.

[4] M. Kyrö, K. Haneda, J. Simola, K. Takizawa, H. Hagiwara, and P. Vainikainen, "Statistical channel models for 60 GHz radio propagation in hospital environments," *IEEE Trans. Antennas Propag.*, vol. 60, no. 3, pp. 1569–1577, Mar. 2012.

[5] P. F. M. Smulders and L. Correia, "Characterisation of propagation in 60 GHz radio channels," *Electronics Commun. Eng. J.*, vol. 9, no. 2, pp. 73–80, Apr. 1997.

[6] M. R. Akdeniz, Y. Liu, M. K. Samimi, S. Sun, S. Rangan, T. S. Rappaport, and E. Erkip, "Millimeter wave channel modeling and cellular capacity evaluation," *IEEE J. Sel. Areas Commun.*, vol. 32, no. 6, pp. 1164–1179, June 2014.

[7] K. Haneda, J. Järveläinen, A. Karttunen, M. Kyrö, and J. Putkonen, "Indoor short-range radio propagation measurements at 60 and 70 GHz," in *Proc. 8th Eur. Conf. Antennas Propag.*, The Hague, The Netherlands, April 6-11, 2014, pp. 717-712.

[8] A. Karttunen, K. Haneda, J. Järveläinen, and Jyri Putkonen, "Polarisation characteristics of propagation paths in Indoor 70 GHz channels," *accepted to the 9th Eur. Conf. Antennas Propag.*

[9] L. J. Greenstein, D. G. Michelson, and V. Erceg, "Moment-method estimation of the Ricean K-factor," *IEEE Commun. Lett.* vol. 3, no.6, pp.175–176, June 1999.

[10] P. Kyösti, et al., "WINNER II channel models", IST-4-027756 WINNER II Deliverable D1.1.2 Part II, V1.0, 2008, online available at [http://www.ist-winner.org/deliverables.html].

[11] C. Gustafson, D. Bolin, and F. Tufvesson. "Modeling the cluster decay in mm-wave channels," in *Proc. 8th Eur. Conf. Antennas Propag.*, The Hague, The Netherlands, April 6-11, 2014, pp. 804-808.

[12] M. Ghoraishi, J. Takada, and T. Imai, "Identification of scattering objects in microcell urban mobile propagation channel," *IEEE Trans. Antennas Propag.*, vol. 54, no. 11, pp. 3473–3480, Nov. 2006.

[13] L. Hentilä, et al. "MATLAB implementation of the WINNER Phase II Channel Model ver1.1." Online: https://www.ist-winner.org/phase_2_model.html (2007) .